RF modulation studies on an S band pulse compressor *

Guan Shu(束冠)[1,2] Feng-Li Zhao(赵风利)[1] Shi-Lun Pei(裴士伦)[1] Ou-Zheng Xiao(肖欧正)[1]

[1] Laboratory of Particle Acceleration Physics & Technology, Institute of High Energy Physics, Chinese Academy of Sciences, Beijing 100049, China
[2] University of Chinese Academy of Sciences, Beijing 100049, China

Abstract: An S band SLED-type pulse compressor has been manufactured by the Institute of High Energy Physics, Beijing, trying to reach 100 MW maximum input power, which means the output peak power is about 500 MW at the phase reversal time. To improve the reliability at very high power, amplitude modulation and phase modulation with flat-top output are considered, and RF modulation studies on the *S*-band SLED are presented in this paper. Furthermore, a method is developed using the CST Microwave Studio transient solver to simulate the time response of the pulse compressor, which can verify the modulation theory. In addition, the experimental setup was constructed and the flat-top output obtained in low power tests. Both amplitude modulation and phase modulation methods can give flat-top output, and the average power gain for both methods is almost the same.

Keywords: S-band, SLED, amplitude modulation, phase modulation, flat-top output, transient solver

PACS: 41.20.-q; 07.57.-c **DOI:** 10.1088/1674-1137/40/3/037002

1 Introduction

SLAC energy doubler (SLED) type pulse compressors play an important role in linear accelerators to increase the efficiency of the klystron RF power. An S band SLED-type pulse compressor has been manufactured by the Institute of High Energy Physics (IHEP), Beijing, to try and reach 100 MW input peak power. During just one compressed pulse time (usually equal to the filling time of the travelling wave accelerating structure) from the incident RF pulse end, the incoming pulse phase is reversed 180° by the PSK (phase shift keying) switcher, and the output peak power will reach 500 MW. The extreme high power leads to sparking around the SLED coupling irises and the first several accelerating cells. A significant reduction of the electric fields near the irises has been achieved by adopting a dual side-wall coupling irises model. High power test results show that the maximum input power can reach 85 MW [1].

To further improve the high power reliability, amplitude modulation (AM) and phase modulation (PM) of the SLED have been considered to decrease the peak power while trying to keep the integrated power over the compressed pulse time at the same level [2–4]. For AM, the input power is slowly increased to compensate the damped radiation power of the storage cavities during the pulse compressed period. For PM, the incoming RF pulse phase is manipulated while the amplitude is kept constant. RF modulation of the SLED is also an effective way to compensate the beam loading effects in multi-bunch operation [5, 6].

In this paper, we present the AM and PM theory based on the equivalent circuit model of the SLED. Inspired by the innovative idea of the CST Microwave Studio (MWS) [7] transient domain simulation developed by Pohang Accelerator Laboratory (PAL) researchers [8], we propose an analogous method to obtain the flat-top output based on the simulation, which can be a verification of the modulation theory. To further confirm our RF modulation study, a low power experimental setup was constructed, in which the flat-top output was achieved.

2 Modulation theory

Figure 1 shows the equivalent circuit model of the SLED. The energy storage cavity can be regarded as an oscillating circuit. The voltage source refers to the RF generator.

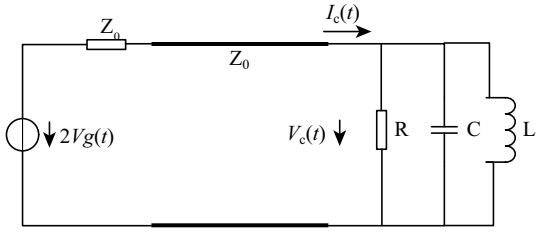

Fig. 1. Equivalent circuit model of the SLED.

Received 1 June 2015, Revised 6 September 2015
∗ Supported by National Natural Science Foundation of China (11475201)

According to Kirchhoff's law, the following differential equation can be obtained (dots mean derivatives with respect to time) [2].

$$V_{\rm r}+\tau\dot{V}_{\rm r}=\Gamma V_{\rm g}-\tau\dot{V}_{\rm g}, \tag{1}$$

where $V_{\rm g}$ is the equivalent complex voltage of the SLED input while $V_{\rm r}$ is the output. $\tau=2Q_1/\omega_{\rm c}$ is the filling time of the storage cavity, Q_1 and $\omega_{\rm c}$ are the loaded Q and the resonant angular frequency. Γ is the reflection coefficient and can be defined as $(\beta-1)/(\beta+1)$ with β the coupling factor.

2.1 AM method

Figure 2 shows the schematic diagram of the AM method. The RF power is fed into the SLED at time t_0, the input phase is reversed by 180° with the amplitude dropping to V_0 at time t_1, and then the incident RF amplitude is modulated (increased continually) to compensate the damped radiation power of the storage cavities until the RF pulse ends at time t_2. During $t_1\leqslant t<t_2$, the output is the superposition of the input power and the radiation power, so the flat-top output can be acquired by an appropriate input waveform.

Conceptually, $V_{\rm g}$ experiences a mutation at times t_0, t_1 and t_2, while the equivalent voltage of the cavity radiation field remain unchanged. Therefore, it can be given that

$$\Delta V_{\rm r}+\Delta V_{\rm g}=0, \tag{2}$$

where $\Delta V_{\rm r}$ and $\Delta V_{\rm g}$ are the transient variation of $V_{\rm r}$ and $V_{\rm g}$ at times t_0, t_1, t_2. The input and output amplitude variations (as shown in Fig. 2) can be calculated by solving Eq. (1) with the boundary condition Eq. (2). In our case, the specifications of the SLED used in the modulation are summarized in Table 1. The theoretical value of the integrated power gain over the compressed interval is 2.25.

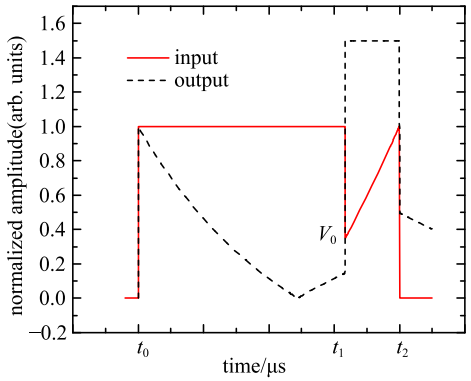

Fig. 2. (color online) Schematic diagram of the AM method.

Assuming the maximum of the input RF amplitude at the end of the pulse is normalized to 1, the output pulse waveform absolutely depends on the V_0 value. Figure 3 shows the input/output field amplitude with three different values of V_0. The solid and dashed lines in Fig. 3 represent the normalized input and output field amplitude, respectively. The situation with V_0=1 corresponds to the original operation mode of the SLED, in which the output has a spike due to a phase reversion. When V_0 is set to 0.6, a partial flat output can be obtained. Furthermore, a full flat-top output can be obtained when V_0 is decreased to 0.3. It can be clearly seen that the peak power at time 3.17 μs and the integrated power over the compressed time is reduced by the AM process.

Table 1. Main parameters of the SLED.

frequency	2998	MHz
resonant mode	$\rm TE_{0,1,5}$	
coupling coefficient	~ 5	
unload Q factor	$\sim 100,000$	
input pulse length	4	μs
output pulse length	0.83	μs

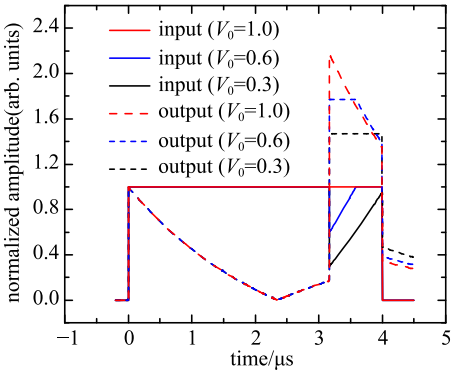

Fig. 3. (color online) Input and output RF amplitude with different V_0.

Figure 4 shows the dependence of the SLED power gain on V_0. Here, the output integrated power over the compressed interval is called the average power. Both the average power and the peak power are reduced by introducing the AM process. However, when V_0decreases from 1 to 0.6, the average power is ∼8% lower than the maximal value, while the peak power is decreased dramatically by ∼33% of the maximum. The sharply reduced peak power can improve the high power reliability significantly. From the point of power utilization efficiency, the partial flat output is more suitable than the full flat-top output [9].

Due to the non-linear input/output characteristics of the klystron at high power, AM performance in the klystron saturation regime will be taken into account in detail.

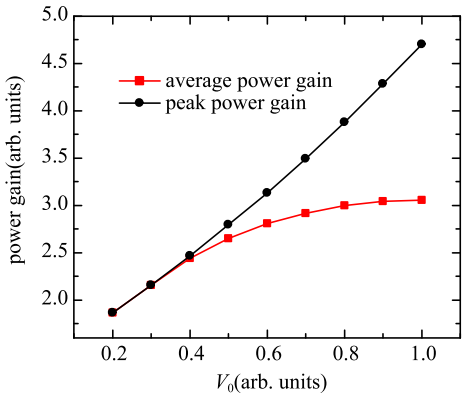

Fig. 4. (color online) Power gain as a function of V_0.

2.2 PM method

Assuming the RF power is fed into the SLED at time t_0, the input has a phase jump with a step φ_0 (generally much less than 180°) at time t_1, then the phase is increased continuously until the RF pulse ends at t_2. The phase modulation based upon the differential Eq. (1) is carried out during $t_1 \leqslant t < t_2$, then a compressed pulse with constant amplitude can be acquired. The detailed formula derivation can be found in Ref. [2]. As is well known, there is a large phase variation in the output during the compressed interval. Figure 5 shows the dependence of the average power gain and the output phase variation on the phase jump step φ_0. The average power gain is proportional to φ_0, while the output phase variation increases with φ_0 as well. For the time duration $t_1 \leqslant t < t_2$, the output phase experiences a large variation. The compressed pulse will be fed into the accelerator structure, and the large phase variation will lead to degradation of the beam performance.

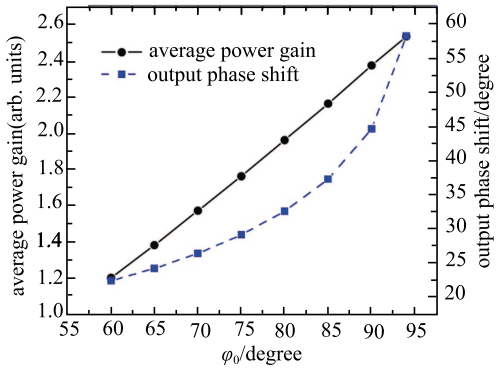

Fig. 5. (color online) Average power gain and output phase variation dependence on the phase jump step φ_0.

In order to reduce the output phase variation, the RF generator frequency can be set at a relatively higher value (e.g. 150 kHz) than the cavity resonant frequency. For this scenario, Eq. (1) can now be modified as follows:

$$V_{\rm r}(1+{\rm j}2\pi\tau\Delta f)+\tau\dot{V}_{\rm r}=(\Gamma-{\rm j}2\pi\tau\Delta f)V_{\rm g}-\tau\dot{V}_{\rm g}, \qquad (3)$$

where $\Delta f = f_0 - f_{\rm c}$ is the frequency shift, f_0 the driven frequency, and $f_{\rm c}$ the resonant frequency of the cavity.

The input and output amplitude and phase variations can be calculated by solving Eq. (3). The specifications of the phase modulated SLED are listed in Table 1. Figure 6 shows the input and output amplitude and phase shapes. At time 3.17 μs, an input RF phase jump of 94° is introduced, and the average power gain with constant output is 2.36. By comparing Fig. 5 and Fig. 6, the output phase variation decreases from several tens of degrees to several degrees.

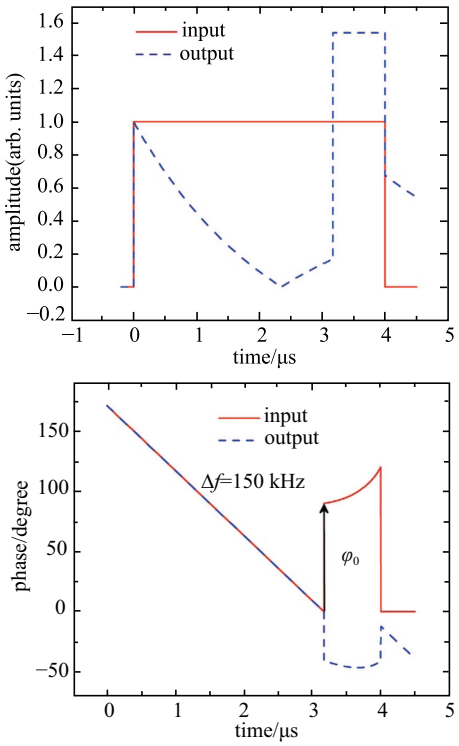

Fig. 6. (color online) Input and output RF amplitude (upper) and phase (lower) variation.

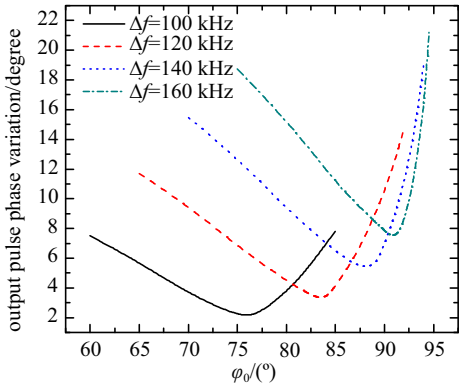

Fig. 7. (color online) Relationship between the output phase variation and the phase jump step φ_0.

The average power gain is proportional to φ_0, so once φ_0 is determined, an optimal value of the frequency shift can be found to minimize the output phase variation, as shown in Fig. 7. Partial flat output can also be acquired by the PM method [10, 11], and the output waveform and power gain are similar to Figs. 3 and 4.

3 Transient simulations

By using the MWS transient solver, the SLED response in the time domain can be studied qualitatively, then the theoretical study results of the AM and the PM can be confirmed. In the case of the AM process, the input pulse is expressed by $V(t)$, sin $(2\pi f_0 t)$ and $V(t)$ is the modulated incident RF amplitude function in Fig. 2. By importing the driven signal shown in Fig. 8(a) into MWS, the SLED response can be simulated, as shown in Fig. 8(b).

For the PM process, the input pulse is expressed by sin $(2\pi f_0 t+\varphi(t))$, f_0 is set 150 kHz higher than the cavity resonant frequency and $\varphi(t)$ is the modulated input phase function in Fig. 6. The driven signal and the SLED response signal simulated by MWS are shown in Fig. 9. The flat-top output is acquired by both AM and PM in the simulation, so this proves the correctness of the theoretical calculations.

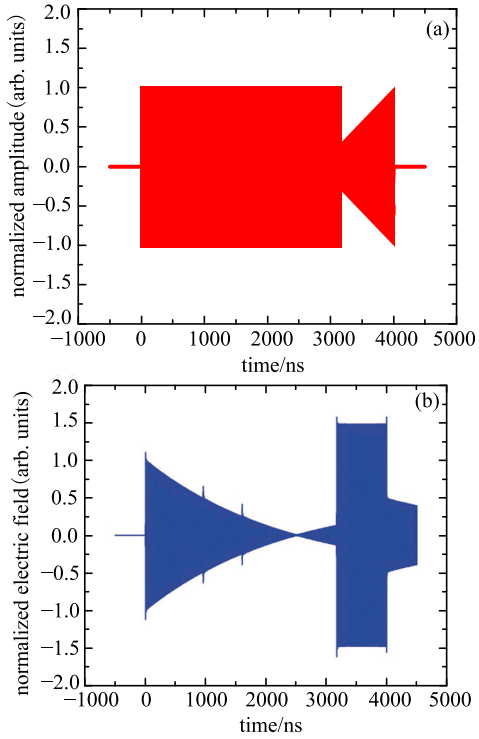

Fig. 8. (color online) (a) driven and (b) response signals of SLED simulated by MWS transient solver with AM method.

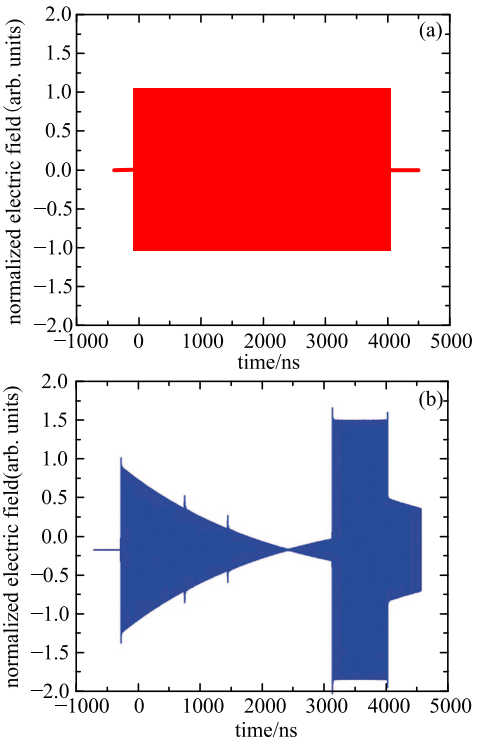

Fig. 9. (color online) (a) driven and (b) response signals of SLED simulated by MWS transient solver with PM method.

4 Experiment

To further confirm our RF modulation study, a low power experimental setup was constructed as shown in Fig. 10. The carrier wave coming from the RF pulse signal generator is modulated by I and Q control levels which are generated by two arbitrary waveform generators. Then the modulated pulse is fed into the SLED cavities. The peak power meter is used to monitor the output.

The parameters of the SLED used in the experiment are given in Table 1. At first, the frequency of the SLED cavities was tuned to $f_0 = 2998$ MHz, then the AM and

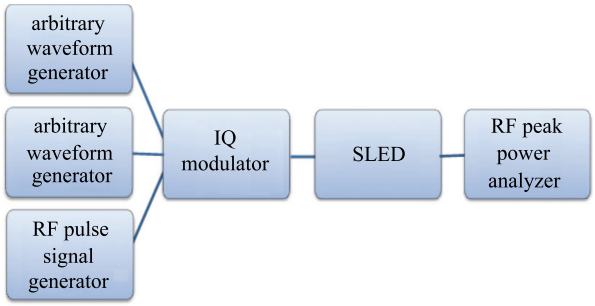

Fig. 10. (color online) Schematic layout of the test.

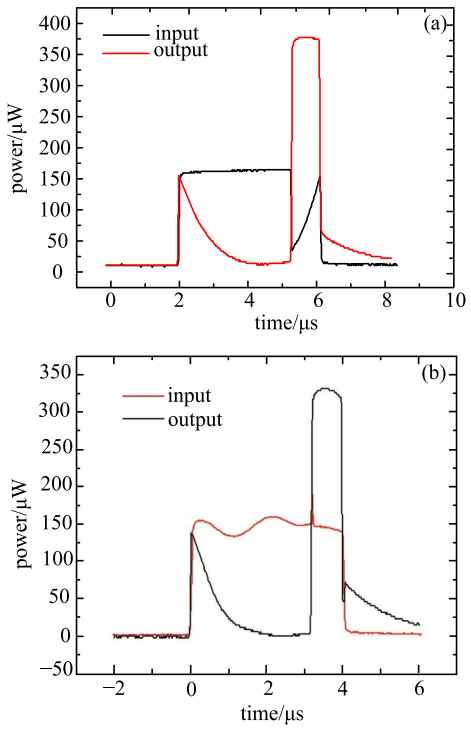

Fig. 11. (color online) Power measurement of the SLED using (a) AM and (b) PM.

PM processes were implemented. Figure 11 shows the cold test results. In the case of the AM, the value of V_0 was set to 0.3 at 3.17 μs, and the flat-top output was obtained as shown in Fig. 11(a). The output average power was 2.33 times the input and the flatness was better than 95%. Figure 11(b) corresponds to the PM method; the RF generator frequency was set as 2998.150 MHz (150 kHz higher than the resonant frequency), and an input RF phase jump of 94 ° was adopted at time 3.17 μs. The flat-top output was obtained with an average power gain of 2.29 and the flatness was better than 95%.

5 Conclusions

An excessive surface field within an RF cavity leads to potentially serious breakdown problems. The maximum RF input power of SLED-type pulse compressors can be enhanced by introducing the RF modulation. We performed AM and PM theoretical analysis, and obtained flat-top output in both the MWS simulation and the low power test. The test shows that the average power gain of the two modulation methods are almost the same. High power tests will be conducted in the future.

References

1 H. Matsumoto, H. Baba, S. Yamaguchi et al, Nucl. Instrum. Methods A, **330** (1) : 1–11 (1993)
2 A. Fiebig, Ch. Schieblich, A SLED Type Pulse Compressor with Rectangular Pulse Shape, in *Proceedings of the 2nd European Particle Accelerator Conference* (Nice, France, 1990), p. 937–939
3 R. Bossart, P. Brown, J. Mourier et al, CERN CLIC-Notes, No. 592, 2004
4 T. Inagaki, 8-GeV C-band accelerator construction for XFEL/SPring-8, in *Proceedings of the 24th Linear Accelerator Conference* (Victoria, Canada, 2008), p. 1090–1094
5 GU Peng-Da, *Studies on New RF Pulse Compressor*, Ph.D. Thesis (Beijing: Institute of High Energy Physics, CAS,1999) (in Chinese)
6 S. Kashiwagi, H. Hayano, K. Kubo et al, Beam loading compensation using phase to amplitude modulation method in ATF, in *Proceedings of the XIX International Linear Accelerator Conference*(1998), p. 91-93
7 Microwave Studio, Computer Simulation Technology, Darmstadt, Germany. www.cst.com
8 Y. Joo, H. Lee, W. Hwang et al, Journal of the Korean Physical Society, **63**(7) :1253–1261 (2013)
9 K. Shirasawa, T. Inagaki, H. Kitamura et al, High power test of c-band accelerating system for Japanese XFEL project, in *Proceedings of the Asian Particle Accelerator Conference* (Indore, India, 2007), p. 2095–2097
10 S. H. Shaker, S. R. Corsini, P. K. Skowronski et al, phase modulator programming to get flat pulses with desired length and power from the CTF3 pulse compressors, in *Proceedings of the International Particle Accelerator Conference* (Kyoto, Japan, 2010), p. 1425–1427
11 C. Serpico, M. Dal Forno, A. Fabris et al, Optimization of the SLED Phase Modulation Parameters of the FERMI Linac, in *Proceedings of the North American Particle Accelerator Conference* (Pasadena, USA, 2013), p. 981–983